In presenting this dissertation as a partial fulfillment of the requirements for an advanced degree from the Georgia Institute of Technology, I agree that the library of the institution shall make it available for inspection and circulation in accordance with its regulations governing materials of this type.

I agree that permission to copy from, or to publish from, this dissertation may be granted by the professor under whose direction it is written, or, in his absence, by the Dean of the Graduate Division when such copying or publication is solely for scholarly purposes and does not involve financial gain.

It is understood that copying from, or publication of, this dissertation which involves potential financial gain will not be allowed without written permission.

Thomas L. Rourk

MODEL STUDIES OF A PILE FAILURE SURFACE IN A COHESIVE SOIL

A THESIS

Presented to

the Faculty of the Graduate Division

by

Thomas L. Rourk

In Partial Fulfillment

of the Requirements for the Degree

Master of Science in Civil Engineering

Georgia Institute of Technology

December, 1961

68
12R

MODEL STUDIES OF A PILE FAILURE SURFACE IN A COHESIVE SOIL

Approved:

George F. Sowers

Aleksandar Vesic

RADNOR J. PAQUETTE

Radnor J. Paquette

Date Approved by Chairman: Jan 3, 1962

ACKNOWLEDGMENTS

The author wishes to express his appreciation to Professor George F. Sowers for the encouragement and guidance rendered throughout the course of this project.

To Professors Aleksandar Vesic and Radnor J. Paquette, thanks are extended for their helpful comments on this text.

To my wife, Ruth, I express deep gratitude for her untiring encouragement, patience and assistance which made the completion of this work possible.

TABLE OF CONTENTS

LIST OF TABLES

LIST OF ILLUSTRATIONS

SUMMARY

The purpose of this investigation was to extend the understanding of pile behavior in cohesive soil by observing the rupture surface developed beneath a forced pile at failure and to correlate the development of the failure plane with the distribution of pile load. This purpose was accomplished by forcing a split pile into a model soil mass constructed of alternate light and dark layers, after which the model was split open and the actual failure plane developed at the end of the pile was observed. SR-4 electronic strain gages, mounted near the pile base, were used to measure the distribution of load. This arrangement provided a measurement of end bearing stress with the remaining share of the total load applied to the model pile assigned to the side bearing.

The results of the tests indicated that the failure of the pile was accompanied by a sudden release of the skin friction along the sides of the pile and the development of local shear planes beneath the pile tip. The test loading was carried beyond the failure point and in no case did general shear failure occur beneath the pile tip.

The application of load to the friction pile produced an immediate end bearing load, after which both the end and side loads increased as the applied load increased with the side load receiving

the greater portion. The load transmitted to the end increased at a slightly increasing rate while the side load increased uniformly.

As the pile approached failure a rapid variation in the relationship between the end and side loads with respect to the total load occurred. A greater portion of the total load was carried in end bearing while less was ascribed to frictional resistance.

It was found that the measured end bearing capacity was approximately forty per cent of the calculated end bearing capacity assuming general shear failure. Since the end bearing capacity of a "friction pile" represents only a small portion of the total bearing capacity a reasonable calculation can be made assuming general shear failure. However, by assuming local shear failure the measured end bearing capacity was found to be approximately fifty-six per cent of the calculated end bearing capacity and thus gives a closer estimate of the bearing capacity.

Further investigations should be directed toward determining the failure surface developed beneath a dynamically placed pile and for a pile placed in a pre-bored hole. Attention should also be given to the soil stresses in the vicinity around the sides and beneath the base of the pile.

CHAPTER I

INTRODUCTION

The rise of modern soil mechanics during the past thirty to forty years has resulted in a safer and more economical use of piles as foundations for larger and heavier structures. However, even with today's advanced methods, derived from experience and exploration of the theoretical aspects of the problem, the design of pile foundations is not yet an exact science.

A pile gains its bearing capacity by transfer of load to the soil by the bearing of its point and side bearing from friction or shear along its surface. A pile that gains most of its load carrying capacity from the bearing of its point is called an "end-bearing pile." When a pile is supported mainly by the friction or shear along its sides it is called a "friction pile." Often, in the case of a friction pile in clay, the point resistance is of minor importance and is therefore neglected; however, for a complete solution this resistance must be considered.

A point bearing failure occurs as a bearing capacity failure of the underlying soil. Three types of failure may occur: general shear failure, local shear failure and a punching failure. The general failure is generally considered to occur in dense or stiff material, local failure in medium dense or plastic material, and punching failure in loose and very plastic material. A failure in

side bearing can occur in one of two ways: first, the soil a small distance from the pile can fail by an actual shear between the soil grains, and second, a failure can occur between the pile sides and the soil.

There are many problems encountered in designing and driving end bearing piles: for example, predetermining adequate length to the point bearing strata and avoiding damage in driving the pile to refusal. In comparison, many of the problems relating to friction piling are more involved, such as the distribution of load from pile to the soil and the reaction of soil around the pile at failure.

The purpose of this research is to extend the investigation of the behavior of piles in homogenous cohesive soil. A model soil mass sample was built with alternate light and dark layers, whereby the actual failure surface developed beneath the pile point for a pile forced in place was observed. Also, by the use of strain measurements, the amount of load contributed to the soil by the pile point was determined.

The cohesive material used in this study was bentonite clay. This is a homogeneous, plastic clay that has no properties of internal friction. This material was used in previous research projects in the Soils Laboratory of the Georgia Institute of Technology.

CHAPTER II

THEORY

The procedure for design of friction piles depends upon the determination of ultimate pile load capacity. A typical load-settlement curve for a pile is shown in Figure 1. The curve shows an initial range where the settlement is approximately proportional to the load. In this range the settlement is due to the elastic distortion and change in volume of the soil around and beneath the pile. Beyond this point a load is reached whereby any further increase in loading results in a substantial increase in rate of settlement. This load is known as the ultimate pile load capacity. In some cases each increment of load produces a proportional amount of settlement up to the failure load where the settlement increases rapidly with no further increase in load. This type of curve is accepted as occurring with general shear failure.

General shear failure in deep foundations is characterized by a definite surface of rupture which begins at the corner of the base and ends at the pile sides (1). The mass of soil involved in shear is very definite.

In other cases the load produces a proportional amount of settlement, but instead of the well-defined failure point occurring, the load-settlement curve continues on at an increasing rate of

slope. This curve is often considered as representing local shear failure (2).

The ultimate pile capacity can be calculated from the soil strength by static analysis (3). This computes the ultimate load of a pile by the sum of the bearing of its point and the friction along its sides. This expression may be written as follows:

$$Q_{ult} = Q_p + Q_s \tag{1}$$

where

Q_{ult} = ultimate pile capacity

Q_p = pile capacity contributed by end bearing

Q_s = pile capacity contributed by skin resistance

The end bearing capacity of a pile may be represented by

$$Q_p = q_p A_p \tag{2}$$

where

q_p = the end bearing capacity of the foundation

A_p = the area of the pile base.

On the basis of plastic theory and with the assumption that the soil is weightless, Meyerhof (4) has shown that the bearing capacity of a deep foundation can be represented by the expression

$$q_p = cN_cE_c + qN_qE_q \tag{3}$$

where c denotes apparent cohesion

q denotes overburden pressure

N_c and N_q denote the bearing capacity factors

E_c and E_q denote shape factors

The bearing capacity factors depend on the angle of internal friction of the soil, the roughness of the pile base and the depth and shape of the pile.

The bearing capacity factors are calculated on the assumption that the soil is a rigid material and general shear failure occurs. However, this is not always the case. The lateral compression of the soil provided by the base may be less than that require to establish plastic equilibrium. In very compressible material the spread of the state of plastic equilibrium is restricted by volume change or displacement and results in local shear failure which in turn reduces the point bearing capacity.

In cohesive material having an internal friction equal zero the bearing capacity can be expressed by the equation

$$q_p = cN_c + q \tag{4}$$

since N_q is equal to one.

Theoretical analysis, assuming general shear failure, has determined the value of the bearing capacity factor including the shape factor, for a deep circular foundation to be 9.7. However, a paper published by Sowers (5) indicates that the factor may be of the order of 9 or even less.

Attempts have been made to determine the bearing capacity factors for local shear failure but none have been successful. One such attempt was made by Bishop, Hill and Mott (6) who found that the factor could be expressed by

$$N_c = \log_e \frac{E_o}{3c} + 2 \tag{5}$$

where E_o denotes modulus of elasticity. However, the results of this approach were found to be too low. At the present time the compressibility of the material may be taken into account by employment of an empirical reduction factor of two-thirds which is applied to the cohesion of the soil.

The skin resistance consists of adhesion and skin friction; however, in soft clay the adhesion is usually the governing factor. The skin bearing capacity may be expressed by

$$Q_s = s\ A_s \tag{6}$$

where A_s denotes the embedded surface area of pile

s denotes the average unit skin resistance.

In cases where the angle of internal friction of the soil is zero and the pile sides are smooth the average unit shearing strength may be expressed as

$$s = c_a \tag{7}$$

where

$$c_a = mc \tag{8}$$

The term c represents the cohesion of the soil and c_a represents the adhesion of pile and soil.

The term m, which is equal to or less than one, represents the coefficient of adhesion which provides the user with a convenient method for using the adhesion when it is less than the shear strength of soil. The term m depends on method of placement and shape of the pile, sensitivity of the clay and amount of thixotropic regain of clay.

By using the static analysis, the pile capacity contributed by skin bearing is computed on the assumption that the skin friction over the embedded length of the pile is equal to either the shear strength of the soil or the adhesion of pile to soil, whichever is the smaller value. According to Seed and Reese (7) and later Wilson (8), the distribution of load along the length of the pile decreases with depth. This leads to the fact that the skin resistance is not uniform over the embedded length of the pile and does not agree with the static formula. However, test results have indicated that this method provides a close approximation to ultimate skin bearing capacity because the error caused by over-estimating the skin resistance at the upper end of the pile is approximately neutralized by the error caused by under-estimating the skin resistance of the lower end of the pile.

A theory of the distribution of applied loads along a pile in soft clay has been stated by Seed and Reese (9). The soil deformation accompanying the downward movement of a rigid pile results in the development of shearing stresses in the soil causing the load in the

pile to decrease with depth. But piles are not completely rigid and the settlement of the top of the pile exceeds the settlement of the bottom of the pile by a distance equal to the elastic compression of the pile. Therefore, the movement of points on pile, which causes soil deformation, decreases with the distance from the pile top and results in shearing resistance of the soil around the pile that causes the load in the pile to decrease with depth. Also, it was concluded that since the soil will deform more readily than the pile, any applied load will always result in some portion being transmitted to the pile tip.

CHAPTER III

APPARATUS

Two model piles were built for the testing program. Both piles were constructed of a thin wall aluminum tubing two inches in diameter and twenty-eight inches long. The first pile was split its entire length and each half fitted with a plug in its base end. The split pile halves were held in place by adjustable water hose clamps. See Figure 2.

SR-4 strain gages were employed to determine the point load of the friction pile. Previous studies by Wilson (10) indicated that reasonable values of end bearing could be obtained by placing strain gages on the sides near the point end of the pile.

With the realization that the strains measured in the point end of the pile would be of a very small magnitude, the cross sectional area of the pile wall was reduced to increase the measurable strain. Starting from the point end of the pile, a three inch long section was machined down to an outside diameter of 1.970 inches providing a wall thickness of 0.015 inches. From this point moving upward, a four inch section was used to taper the pile to its original diameter. Two holes were drilled near the top for bringing out the lead wires from the gages. See Figure 3.

Four A-8 paper back strain gages, having a nominal gage length of one-eighth inch, were placed inside the pile in opposite corners

approximately one-fourth inch from the point end. The gages were installed as follows: The interior surface of the pile was prepared by roughening it with emery cloth and then scrubbing it with acetone using clean cotton. Next, a liberal amount of Duco cement was applied to the surface and the gage was properly placed. A piece of cellophane was placed over the gage to prevent its sticking to any object. Then, a piece of felt was used to spread the load of a one pound weight evenly over the gage. Due to the thickness of the gages, they were allowed to dry forty-eight hours at room temperature. A microcrystalline wax known as Petrosene was then applied to waterproof the gage. A dummy gage was installed in another piece of tubing to compensate for temperature effects on strain readings.

When all gages had been installed in the pile, a volt-ohm micro-ammeter was used to check for correct gage resistance and for resistance to leakage from the gage to the metal sides of the pile. All gages indicated one hundred-twenty ohms resistance.

An aluminum base plate one eighth inch high with a one-sixteenth inch recessed portion was sealed to the pile end with Petrosene wax. An aluminum loading plate was constructed with a recessed groove to act as the pile cap for both piles. The plate acted to hold the two halves of the split pile concentric and to evenly distribute the load. Before placing the piles, the outside walls were rubbed with emery cloth and sprayed with clear lacquer to prevent any reaction from occurring between the aluminum and the bentonite.

Strain readings were made using a Type N Baldwin Portable SR-4 Strain Indicator. Readings were possible to one micro-inch per inch. In addition, a Baldwin SR-4 Switching and Balancing unit was used in conjunction with the indicator to provide for the initial balancing of the gage bridge to zero.

The material used in testing was a bentonite clay that had been used in previous tests at Georgia Institute of Technology. Bentonite forms a thixotropic gel with water and results in a homogeneous, highly plastic, cohesive material. After being completely remolded, the material has the ability to regain its shear strength in about five days. This was a very desirable characteristic in that the individually placed layers re-gel to form a homogeneous mass.

To obtain the stiffest, workable mixture of water and bentonite several trial mixes were made. A mix with a water content of three hundred per cent was found most suitable. Mixes with lower water contents were found to contain numerous air voids which were hard to eliminate from the sample.

After trying several admixtures, it was found that mixing the bentonite with commercial lampblack provided a suitable dark material for the layered model. A quantity of 0.2 per cent by total weight of lampblack was mixed into the bentonite using the large mechanical mixer in the Soils Lab.

The layers for the bentonite model were formed in molding rings. These were machined aluminum rings one-half inch high with a

twelve inch inside diameter. The container for the bentonite was Sonotube which is a commercial product used in forming concrete columns. This provided a stiff cardboard water proof jacket which was easily cut with a skill saw. The jacket used had an inside diameter of twelve inches.

The base for the sample consisted of a one-fourth inch steel plate with an attached vertical rod for the purpose of measuring the pile settlement. The base further consisted of two three-fourth inch plywood plates. The bottom plate was one piece to allow movement of the model on the steel plate. The top plate was split in two pieces allowing the sample to be cut in half. The two halves of the top plate were held in place by four one-fourth inch metal dowels that extended to the bottom base plate. The dowels acted to hold the two halves in place and insure proper alignment of the pile and layered sample.

The piles were forced into the bentonite using a screw-operated driving device. This consisted of a simple screw with a thrust bearing at the end. Load was applied to the test piles by the Tinus Olsen Universal Testing Machine in the Soils Laboratory of the Georgia Institute of Technology. The testing machine provided a constant strain type of loading capable of one pound load increments.

CHAPTER IV

PROCEDURE

Several preliminary tests were conducted with a surface loaded model. These tests were used to devise a method for making a bentonite model with alternate light and dark layers and to observe the effects of failure of the foundation without disturbing the resulting shear surfaces.

The preliminary tests were performed in a split steel mold fitted with lugs to allow the sample to be cut in half. The bentonite was placed in one-half inch light and dark layers in the split mold and allowed to regel for a five day period. A split footing, two inches in diameter, was used to apply the surface loads. The footing was coated with lacquer before testing.

Using the testing machine, load was applied to the footing until failure. The model was then cut open by passing a wire saw through the mold, and the two sections were separated. Thus, the failure surface developed by the downward movement of the footing was observed without being disturbed.

It was also found that the test could be interrupted at a desired increment of settlement for the failure surface to be observed. The model would then be closed and the test carried to the next increment of settlement where any further development in the

failure surface could be observed. This procedure appeared to have no visible effects on the development of the failure surface.

The testing program for thepile tests consisted of two separate procedures. The first test was designed to observe the failure surface of a pile in cohesive soil. The bentonite model consisted of sixty light and dark layers. The individual layers were formed in the one-half inch deep molding rings with care being taken to eliminate all air voids. After forming, the ring and bentonite layer were placed in the correct position on the base plate and a very thin knife edge was passed around the inside of the ring to break the adhesion of the bentonite to the mold to allow removal of the ring. This procedure was repeated, stacking the light and dark layers alternately until the model reached a height of fifteen inches. A Sonotube jacket was then placed around the model and tightly strapped with adjustable clamps and masking tape. Another fifteen inch section was placed on the first, bringing the total height of the sample to thirty inches.

The pile was forced to a depth of twenty inches using the screw-operated loading device. In the process of forcing, the exposed portion of the split pile was held in place with adjustable clamps while the portion within the bentonite was held in place by the pressure exerted by the material on the sides of the pile. This method held the pile halves in place during the placing and testing of the model.

After allowing the bentonite a five day re-gel period, the test of the pile model was begun. The model, sitting on its base, was placed in the loading machine and load was applied until a settlement of ten per cent of the diameter of the pile was reached. This increment of settlement will be designated Pile Test 1. The model was removed from the loading platform and prepared for opening. A wire saw was carefully passed through the split pile, layered sample and split sides of the jacket. This was accomplished with difficulty because the pressure exerted on the sides of the pile was great enough to hinder the downward movement of the saw. With the sample cut in two, the metal dowels were removed from the base and half the model was removed by sliding half of the split base outward.

The failure surface was observed and the model was replaced on its base. The dowels were placed in their respective holes in the base plates to insure perfect alignment of pile and sample. The pile was reloaded to settlement increments of twenty, thirty, and fifty per cent of the diameter of the pile with observations made after each increment of settlement. The tests will be respectively designated as Pile Tests 2, 3, and 4.

In the second group of tests, strain gages were used to measure the amount of load contributed to the soil by the pile point. Before placing the pile in the bentonite, the strain gages were calibrated. The gages were checked and then connected to the strain indicating equipment. Loads of approximately three times the estimated point load were applied and removed using the testing

machine. This loading and unloading was repeated until the strain readings became constant.

Under identical loading conditions and various pile positions, the strain gages repeated themselves to within three micro-inches per inch. Several loadings were performed and the average strain readings were plotted versus the load which resulted in a linear variation.

The bentonite model was built in the same manner as in the first test with the exception of one inch layers being used. The model was not constructed of light and dark layers since the failure surface was not to be observed.

Load tests were performed on the model pile for embedded lengths of sixteen inches, twenty inches and twenty-four inches, designated respectively as Pile Tests 5, 6, and 7. The varying depths were tested to check the results and to determine the variation of point load with the depth of embeddment. At designated values of total load the value of pile settlement and the resulting strain readings were recorded. A five day re-gel period was allowed between each test.

The shear strength of the bentonite was determined using a miniature vane shear apparatus. The torque to rotate the vane was applied by a conventional torque wrench calibrated in torque increments of one inch-pound. Shear tests were performed at the surface and at the base of the pile for all models.

A pull test was used to determine the adhesion between the bentonite and the pile. A piece of aluminum tubing was prepared and

forced into a container of bentonite using the same procedure as for the model piles. The bottom of the tubing was flush with the base of the mold which was not enclosed. Thus, the bentonite surrounded the sides of the pile but did not enclose the base. This eliminated the possibility of a vacuum's being created at the pile base caused by its upward movement.

CHAPTER V

DISCUSSION OF RESULTS

The purpose of this study was to advance the present state of knowledge concerning the action of piles in cohesive soil. The tests resulted in information concerning the actual failure surface for both shallow and deep foundations and the distribution of pile load in soft clay.

The first series of tests was conducted in the form of preliminary studies to define the failure plane of a shallow foundation. All surface tests resulted in failure of the footing by local shear failure.

Failure planes were observed extending downward from the corners of the footing at an angle of forty-five degrees with the base. Theoretically this is in agreement for soils having an angle of internal friction equal zero. The material within this wedge was undisturbed by the downward movement and was obviously in a state of elastic equilibrium. This wedge will hereafter be referred to as Zone I.

The failure planes extended outward from the point of intersection of the planes forming Zone I but did not move upward toward the surface as expected in general shear failure. According to Terzaghi, "In cohesive soil the surface of sliding terminates at the boundary of the zone of elastic equilibrium." (11) The lateral

distortion produced by the downward movement of the footing was less than the lateral distortion required to spread the zone of plastic equilibrium outward and upward to the surface. Thus the failure planes extended to the limits of the zone of plastic equilibrium where they stopped and resulted in failure by local shear.

The load-settlement curves for the tests, shown in Figure 8, were regarded as typical curves accompanying a local shear failure. The curves first deviated from the initial straight line portion of the curve at approximately two per cent of the diameter of the footing, with the failure load occurring roughly between four to five per cent of the diameter of the footing.

The measured ultimate load bearing capacity of the surface foundation was considerably less than the calculated bearing capacity using the Meyerhof analysis, whereby 6.14 was used as the bearing capacity factor. However, by making the empirical reduction in the shear strength necessary with the occurrence of local shear failure, the calculated bearing capacity compared reasonably with the measured bearing capacity. The comparative bearing capacity values for the surface tests are given in Table 11. The average per cent measured bearing capacity of the calculated value was found to be approximately seventy. The fact that the measured bearing capacity is still less than the calculated value indicates the need for bearing capacity factors that depend upon the elasticity of the material. Bearing capacity factors depending upon the elasticity of the material would also eliminate trying to predict the occurrence of local shear failure.

The empirical reduction used for compressible soil obviously covers only a small range of materials; however, as indicated by these tests, the results are not unreasonable.

The failure surface for the deep foundation was observed after the settlement had been carried to ten per cent of the diameter of the pile. The Zone I wedge beneath the pile point was fully developed and also failure surfaces were visible, progressing outward from the point of Zone I. The failure surface developed appeared as a typical local shear failure quite similar to that developed in the shallow foundation test. See Figure 4.

The testing was continued with the model being opened at increments of settlement corresponding to twenty, thirty and fifty per cent of the diameter of the pile. The failure surfaces were observed and were found to remain relatively unchanged with increase in settlement. The Zone I wedge was fully developed at the first opening and did not change in shape with increase in penetration. The failure surfaces extending outward from the point of Zone I moved progressively downward with pile movement and did not change in shape nor length.

It is apparent from the load-settlement curves, shown in Figure 9, that opening the model for observation had very little effect on the bearing capacity of the pile. There was a reduction of approximately five per cent in ultimate load bearing capacities of Test 1 and 2 which was probably caused by remolding of the clay and not opening the sample.

The Zone I wedge found beneath the pile was formed by failure surfaces extending downward from the corners of the base at an angle of forty-five degrees. This is in agreement with the theory of failure and similar to that found in the shallow foundation tests. Zone I consists of relatively undisturbed material taken from the top two layers and a portion of the third. The wedge accompanied the pile base downward from the surface with little disturbance which indicates that the material was in a state of elastic equilibrium.

The development of the failure surfaces beyond the point of Zone I was found to be that of a typical local shear failure. From Figure 5, it is apparent the planes moved outward but it is not visibly apparent as to how far they extend out from the pile. However, the failure surfaces definitely did not extend upward to the sides of the pile as expected in general shear failure.

The occurrence of local shear failure for the deep foundation was also attributed to the low elasticity of the bentonite. The downward movement of the pile produced a lateral distortion which resulted in a reduced zone of plastic equilibrium. Thus, the failure surface terminated at the edge of the zone of plastic equilibrium and local shear failure occurred.

The soil immediately surrounding the pile sides and Zone I was disturbed by the downward movement of the pile. The point where each layer deflected from its original horizontal position indicated the zone of influence created by the pile. These points were plotted

and the zone of pile influence is shown in Figure 6. The zone extended approximately one pile diameter outward from the sides of the pile and approximately two pile diameters below the pile point.

The penetration of the pile into the soft clay caused the layers to be dragged down by the sides of the pile. The downward movement of the pile caused the layers below the base to stretch in a downward direction from their original horizontal position. This downward stretching or pushing was initially under elastic conditions, but as the pile approached the layer it entered the zone of plastic equilibrium and the layer was sheared by the failure plane. The point of Zone I passed through the layer and the separated ends drifted along the sides of Zone I, and then along the pile as it proceeded downward.

This action explains the rebound of the pile. The rebound is attributed to the action of the elastically distorted layers beneath the pile point. As the load was removed from the pile, the layers created an upward force in their attempt to return to their original position, thus, causing an upward force on the pile base which caused a negative skin friction on the sides of the pile.

The first load distribution test was conducted on the model pile at a depth of eight pile diameters. After the pile was forced in place, the sample was allowed to re-gel for a five day period. At the end of this period an upward force on the pile point was indicated by the strain indicator. In observing the layered model sample, the layers were seen to be stretched or deflected downward by the pressure

exerted from the base of the pile. This pressure was greatest at the edge of Zone I where the soil was in plastic equilibrium. Beyond this zone the magnitude of the pressure exerted on the soil became smaller with increase in distance from the pile; thus, placing a portion of the material in elastic equilibrium. Therefore, the upward force exerted on the pile point was caused by elastically compressed material trying to return to its original position. This upward force was observed in all tests.

The upward force on the pile point indicated that the forces of side resistance must act in the opposite direction for the pile to be in equilibrium in the unloaded condition. No attempt was made to accurately measure the upward force on the pile which had been done previously by Fausold (12); however, the loads indicated a slight increase in magnitude with increase in depth of the pile. The upward force decreased during the re-gel period which was a result of thixotropic regain in strength of the material.

The application of load to the test piles produced an immediate effect upon the base of the pile. This is in agreement with the theory of Seed and Reese (9) which concludes that the difference in the elastic deflection of the pile and soil permit an immediate transfer of a portion of the total pile load to the base.

The end load increased with the increase in pile load but the portion of the load transmitted to the end was small as compared to that received by the sides. This is illustrated by Figures 11 through 13 showing the total load versus end and side load. The side load can

be seen increasing at a much greater rate than the end load. Results similar to these were previously found by Fausold (13).

All the figures illustrating the variation in distribution of total load between the end and side resulted in a straight line variation for the side load. However, the line representing end load was slightly concaved upward. This indicates that load transmitted to the base increased at a slightly increasing rate as the loading progressed.

As the pile stress approached failure a rapid variation in the relationship between the end and side load with respect to the total load occurred. The curve showing end bearing indicated that the value of end load increased rapidly with the maximum slope occurring at the point of failure. The proportion of the total load received by the sides of the pile suddenly approached a constant or slightly reduced value at failure. Further examination of the loads received by the end and sides revealed that at failure the end received approximately seventeen per cent of the total load and the sides received approximately eighty-three per cent. The test loading was continued beyond the point of failure with the curve of skin friction continuing at a constant value and the end load indicating a very slight increase.

As indicated by the load-settlement curves in Figure 10, the point of failure was very well defined. The curves first deviated from their initial tangent at roughly two per cent of the pile diameter, which is the same point as for shallow foundations, with failure occurring between three to four per cent of the diameter of the pile.

This type curve is generally accepted as representing general shear failure; however, this type failure did not occur as indicated by previous results. Therefore, the load-settlement curve must represent the failure characteristics of the skin resistance. The failure occurred suddenly as a release of the skin resistance between the pile and the soil. This type failure was probably caused by the sensitivity of the bentonite.

Comparative results of calculated and measured bearing capacities for the pile tests are given in Table 11. The bearing capacities for both general and local shear failure are given in comparison to the measured. Using values of coefficient of adhesion equal 0.513 and bearing capacity factor equal 9.0, the measured bearing capacity was found to vary from eighty-three to seventy-seven per cent of the total load calculated assuming general shear failure and ninety-four to eighty-four per cent assuming local shear failure with a bearing capacity factor equal 6.0. All values were found to decrease with increase in depth. Since the value of the side load remains constant in both sets of calculations, the reason for the variation lies in the determination of the end load. Assuming general shear failure using a bearing capacity factor equal 9.0, the per cent measured of calculated values for the end loads varied from forty-three to thirty-seven per cent with values varying from sixty-one to fifty-five per cent assuming a bearing capacity factor equal 6.0 for local shear failure with all the values decreasing with depth. In comparing the per cent measured of calculated values for general shear failure and local shear failure

it was apparent that the difference in percentages for the total load was relatively smaller than the end load. This is a result of the small percentage of the total load contributed by the end load for a friction pile. This, coupled with the fact that the percentage of end load decreases with increase in depth, resulted in the conclusion that a calculation within forty per cent of the actual can be made to determine the end bearing capacity of a friction pile in compressible material with the angle of internal friction equal to zero by assuming general shear failure. However, if local shear failure is assumed the calculation will be approximately fifteen per cent closer to the actual end bearing value. This is not true in shallow foundations where the only load is that of end bearing.

The vane shear tests performed resulted in an average shear strength of 0.865 pounds per square inch. It was realized that this value would be larger than the "friction" developed between the pile and the clay and therefore be the controlling factor in the determination of the load carried in "friction." A pull test was used to determine the average value of adhesion of the pile and soil. An aluminum tube with the same diameter and exterior finish as the model piles was pulled from a mold where the only force resisting the pull was the friction developed between the sides of the tubing and the soil. The test resulted in an average value of 0.444 pounds per square inch. The average measured value, shown in Table 12, was found to be 0.443 pounds per square inch. From this value the coefficient of adhesion was found to be 0.513. The pull test obviously

rendered a good average representation of the skin resistance developed along the sides of the pile.

According to Wilson (6) the friction developed along a pile shaft is not a constant value, but becomes greater with increasing depth. Therefore, the value obtained in the pull test was only an average approximation between the maximum and minimum values of skin friction developed along the pile.

The close approximation of the adhesion value resulted in the measured side bearing capacity comparing very closely with the calculated value. The per cent measured of the calculated value was found to be approximately ninety-seven.

CHAPTER VI

CONCLUSIONS

1. The shallow foundation in soft clay failed by local shear failure with the ultimate load bearing capacity occurring at a settlement corresponding to approximately four to five per cent of the diameter of the footing.

2. The empirical reduction factor of two-thirds should be used in estimating the bearing capacity for a shallow foundation in compressible material.

3. Local shear failure occurred beneath the pile base with the failure along the pile sides occurring as a sudden release of skin resistance. The ultimate pile bearing capacity occurred at a settlement corresponding to three to four per cent of the pile diameter.

4. An upward force was found to acton the base of the forced but unloaded pile. This force, which is reduced as time progresses, was caused by the rebound of the elastically compressed clay beneath the base of the pile.

5. The application of load to the friction pile produced an immediate effect upon the end load.

6. Both the end and side load for the friction pile increased with the application of load; however, the side received the greater share of the load. The load transmitted to the end increased at a slightly increasing rate while the side load increased uniformly.

7. As failure approached, a greater portion of the total load was received in end bearing while less was attributed to frictional resistance.

8. A reasonable calculation can be made to determine the end bearing capacity of a friction pile in compressible material having an angle of internal friction equal zero, by assuming general shear failure. However, if local shear failure is assumed the calculation will be closer to the end bearing value.

9. The pull test provided an accurate method of obtaining an average approximation of the skin friction developed along the sides of the pile.

10. The coefficient of adhesion for the bentonite clay and the aluminum pile was found to be 0.513.

CHAPTER VII

RECOMMENDATIONS

1. Investigations should be directed toward determining the failure surface developed beneath a dynamically placed pile and for a pile placed in a pre-bored hole.

2. Efforts should be directed toward an investigation of soil stresses in the vicinity around the sides and beneath the base of the pile.

A P P E N D I X

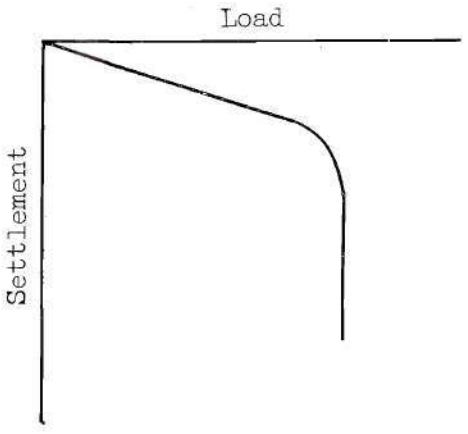

Figure 1. Typical Load-Settlement Curve

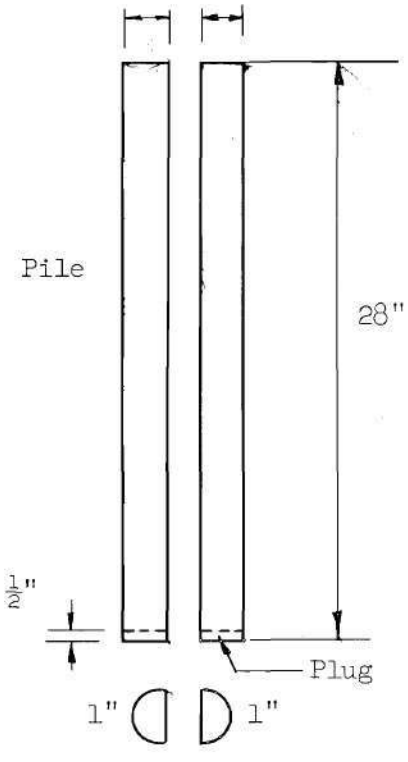

Figure 2. Split Pile Diagram

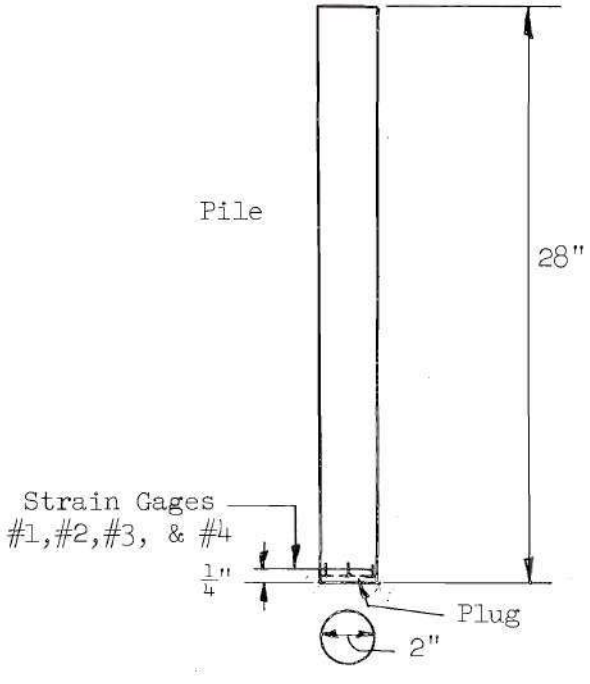

Figure 3. Gage Pile Diagram

Table 1. Surface Load Test Results

Load (pounds)	Test 1 Deflection (inches)	Test 2 Deflection (inches)	Test 3 Deflection (inches)
0.0	0.000	0.000	0.000
0.5	0.003	0.003	0.004
1.0	0.007	0.006	0.007
1.5	0.011	0.009	0.010
2.0	0.014	0.013	0.013
2.5	0.018	0.017	0.016
3.0	0.022	0.021	0.019
3.5	0.026	0.025	0.022
4.0	0.030	0.031	0.025
4.5	0.034	0.035	0.030
5.0	0.039	0.041	0.033
5.5	0.043	0.046	0.040
6.0	0.050	0.054	0.047
6.5	0.057	0.062	0.056
7.0	0.063	0.071	0.071
7.5	0.072	0.082	0.095
8.0	0.088	0.011	0.120
8.5	0.138	0.015	0.166
9.0	0.222	0.207	0.200

Weight of Footing = 0.27 pounds

Table 2. Pile Test: Observation of Failure Surface

Load (pounds)	T Test 1 Settlement (inches)	Test 2 Settlement (inches)	T Test 3 Settlement (inches)	Test 4 Settlement (inches)
0	0.000	0.162	0.364	0.562
5	0.002	0.165	0.366	0.566
10	0.006	0.168	0.369	0.569
15	0.009	0.170	0.372	0.572
20	0.013	0.174	0.376	0.575
25	0.016	0.176	0.379	0.578
30	0.019	0.179	0.382	0.581
35	0.022	0.183	0.386	0.585
40	0.026	0.186	0.390	0.590
45	0.031	0.190	0.393	0.593
50	0.036	0.193	0.398	0.599
55	0.043	0.199	0.404	0.607
60	0.065	0.282	0.510	0.689
61	-	0.400	0.600	1.000
61.5	0.200	-	-	-
50	0.197	0.396	0.596	0.996
40	0.191	0.391	0.590	0.990
30	0.186	0.385	0.584	0.983
20	0.179	0.379	0.578	0.978
10	0.171	0.373	0.570	0.971
0	0.162	0.364	0.562	0.963

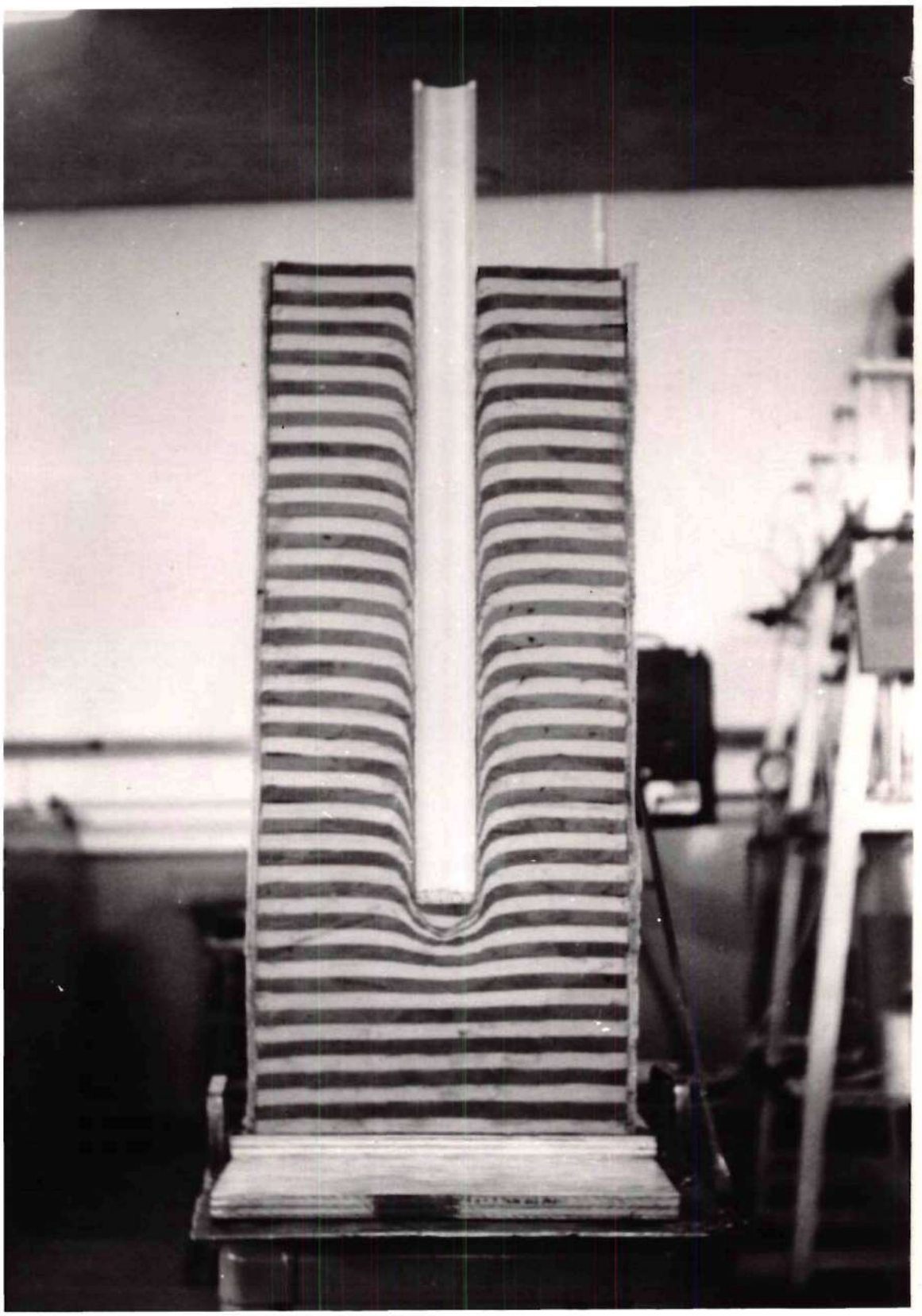

Figure 4. Effect of Forced Pile on Soft Clay

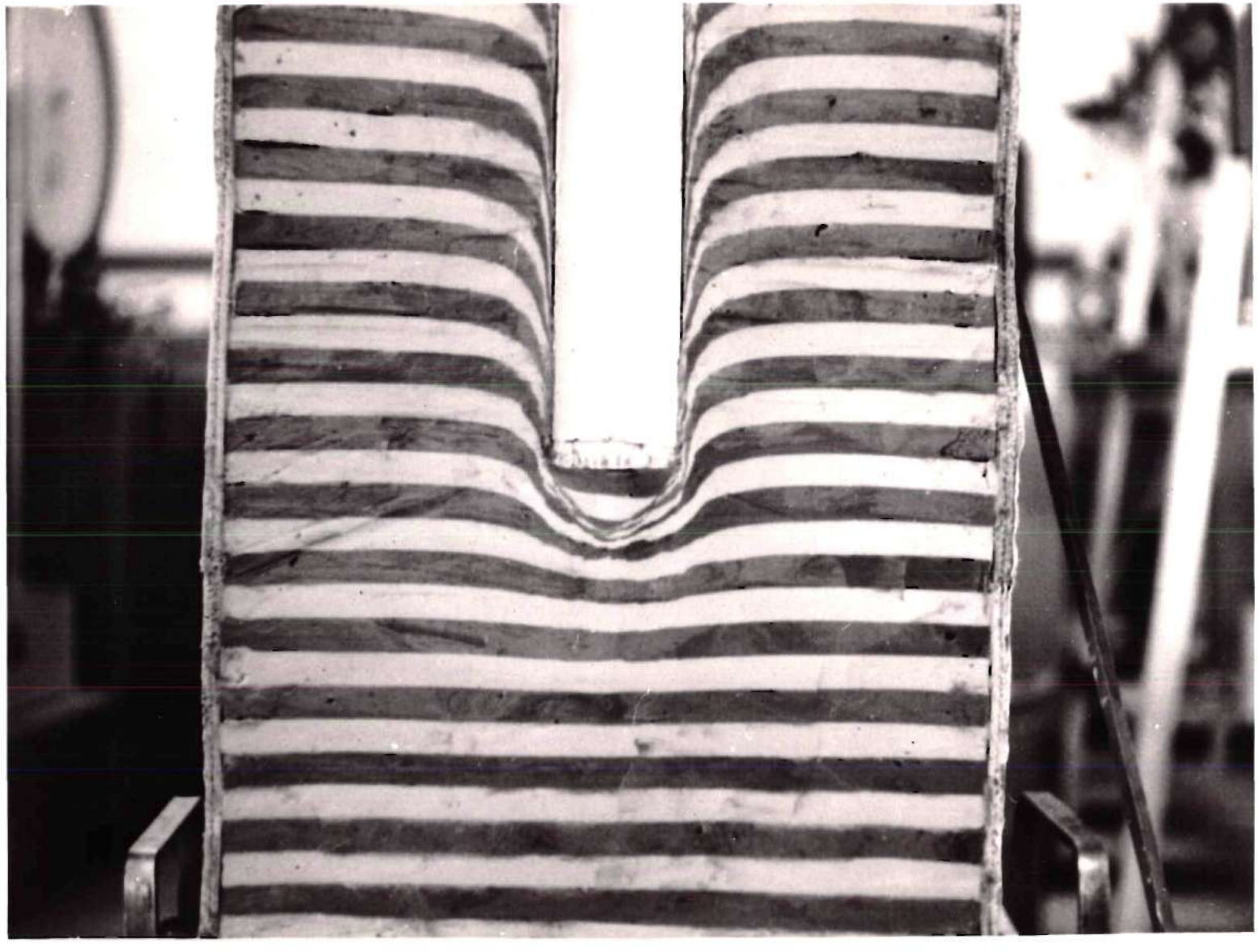

Figure 5. Failure Plane Developed Beneath Forced Pile

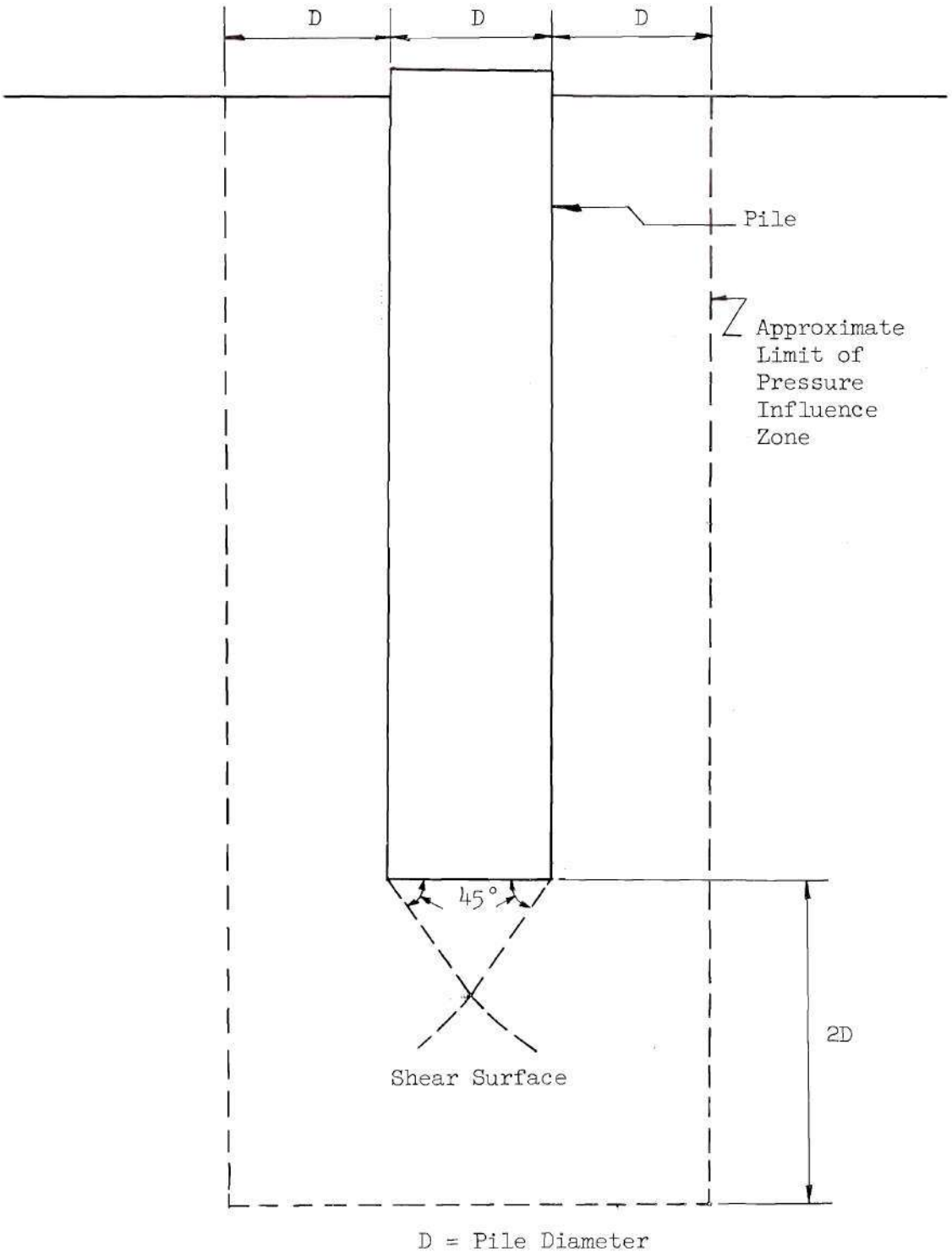

Figure 6. Pile Pressure Influence Zone.

Table 3. Pile Test 5: Determination of Point Load

(Data Sheet)

Depth of Embeddment: 16 inches

Load (pounds)	Deflection (inches)	Strain Gage #1 (micro-in/in)	Strain Gage #2 (micro-in/in)	Strain Gage #3 (micro-in/in)	Strain Gage #4 (micro-in/in)
0	0.000	1	1	1	1
5	0.003	1	2	1	2
10	0.007	2	2	2	2
15	0.010	2	2	2	2
20	0.013	2	2	2	2
25	0.015	2	2	2	2
30	0.019	2	3	2	2
35	0.022	2	3	3	2
40	0.025	3	4	3	3
45	0.029	3	4	4	3
50	0.033	4	4	5	4
55	0.037	4	5	6	6
57.5	0.042	6	7	7	6
57.5	0.070	6	7	7	7
0	-	3	3	3	3

Table 4. Pile Test 6: Determination of Point Load

(Data Sheet)

Depth of Embeddment: 20 inches

Load (pounds)	Deflection (inches)	Strain Gage #1 (micro-in/in)	Strain Gage #2 (micro-in/in)	Strain Gage #3 (micro-in/in)	Strain Gage #4 (micro-in/in)
0	0.000	1	2	1	1
5	0.005	1	2	2	2
10	0.008	2	2	2	2
15	0.010	2	2	2	2
20	0.013	2	2	2	2
25	0.015	2	2	2	2
30	0.018	2	2	2	2
35	0.021	2	3	2	3
40	0.024	2	3	2	3
45	0.027	3	3	3	3
50	0.030	3	4	3	3
55	0.034	4	4	4	4
60	0.038	6	5	4	5
63	0.045	7	7	7	7
63	0.070	7	7	7	7
0	0.070	3	4	3	3

Table 5. Pile Test 7: Determination of Point Load

(Data Sheet)

Depth of Embeddment: 24 inches

Load (pounds)	Deflection (inches)	Strain Gage #1 (micro-in/in)	Strain Gage #2 (micro-in/in)	Strain Gage #3 (micro-in/in)	Strain Gage #4 (micro-in/in)
0	0.000	2	2	1	2
5	0.003	2	2	1	2
10	0.005	2	2	1	2
15	0.007	2	2	2	2
20	0.009	2	2	2	2
25	0.011	2	3	2	3
30	0.014	3	3	3	3
35	0.016	3	4	3	3
40	0.018	4	4	4	4
45	0.021	4	4	4	4
50	0.023	4	4	4	4
55	0.026	4	5	4	4
60	0.030	4	5	5	5
65	0.034	5	6	5	6
70	0.043	6	6	6	6
71	0.051	7	8	8	8
71	0.070	8	9	8	8
0	-	3	3	4	3

Table 6. Pile Test 5: Determination of Point Load

(Load Distribution)

Depth of Embeddment: 16 inches

Load (pounds)	Deflection (inches)	Average Strain (micro-in/in)	End Load (pounds)	Side Load (pounds)
0	0.000	1.0	2	-2
5	0.003	1.5	2	3
10	0.007	2.0	3	7
15	0.010	2.0	3	12
20	0.013	2.0	3	17
25	0.015	2.0	3	22
30	0.019	2.2	3	27
35	0.022	2.5	4	31
40	0.025	3.2	5	35
45	0.029	3.5	5	40
50	0.033	4.3	6	44
55	0.037	5.3	8	47
57.5	0.042	6.5	10	47.5
57.5	0.070	6.8	10+	47
0	-	3.0	5	-5

Weight of Pile = 1.70 pounds

Table 7. Pile Test 6: Determination of Point Load

(Load Distribution)

Depth of Embeddment: 20 inches

Load (pounds)	Deflection (inches)	Average Strain (micro-in/in)	End Load (pounds)	Side Load (pounds)
0	0.000	1.2	2	-2
5	0.005	1.8	3	2
10	0.008	2.0	3	7
15	0.010	2.0	3	12
20	0.013	2.0	3	17
25	0.015	2.0	3	21
30	0.018	2.0	3	27
35	0.021	2.5	4	31
40	0.024	2.5	4	36
45	0.027	3.0	5	40
50	0.030	3.3	5	45
55	0.034	4.0	6	49
60	0.038	5.0	8	52
63	0.045	7.0	10	53
63	0.070	7.0	10	53
0	-	3.3	5	-5

Weight of Pile = 1.70 pounds

Table 8. Pile Test 7: Determination of Point Load

(Load Distribution)

Depth of Embeddment: 24 inches

Load (pounds)	Deflection (inches)	Average Strain (Micro-in/in)	End Load (pounds)	Side Load (pounds)
0	0.000	1.8	3	-3
5	0.003	1.8	3	2
10	0.005	1.8	3	7
15	0.007	2.0	3	12
20	0.009	2.0	3	17
25	0.011	2.5	4	21
30	0.014	3.0	5	25
35	0.016	3.3	5	30
40	0.018	4.0	6	34
45	0.021	4.0	6	39
50	0.023	4.0	6	44
55	0.026	4.3	6	49
60	0.030	4.8	7	53
65	0.034	5.5	8	57
70	0.043	6.5	9	61
71	0.051	7.8	12	59
71	0.070	8.3	12+	58
0	-	3.3	5	-5

Weight of Pile = 1.70 pounds

Table 9. Vane Shear Test Results

Test Group Average	Torque (in-lbs)	Shear Strength (lbs/in^2)
1	4	1.092
2	3	0.820
3	3	0.820
4	3	0.820
5	3	0.820
6	3	0.820

Average Shear Strength = 0.865 lb/in^2

$$S = \frac{T}{\pi d^2 (h/2 + d/6)}$$

s = shear strength (lbs/in^2)

T = torque (in-lbs)

d = diameter of vane (inches)

h = height of vane (inches)

Table 10. Adhesion Test Results

Test	Area of Tubing Side (in^2)	Weight of Tubing (pounds)	Pull Load (pounds)	Adhesion (lbs/in^2)
1	50.27	3.19	26.50	0.455
2	50.27	3.19	25.40	0.442
3	50.27	3.19	25.10	0.436

Average Adhesion = 0.444 lb/in^2

Table 11. Comparative Relationships Between Calculated and Measured Bearing Capacities

Theoretical Bearing Capacity Factors		Average Measured Bearing Capacity Factors
General Shear Failure	Local Shear Failure	
	Surface Tests	
6.14	4.11	2.94
	Pile Tests	
9.00	6.00	3.94

Table 11. (Continued)

Test	Calculated Bearing Capacity (pounds)						Measured Bearing Capacity (pounds)		
	General Shear Failure			Local Shear Failure					
	Point	Side	Total	Point	Side	Total	Point	Side	Total
				Surface Tests					
#1	16.7	-	16.7	11.1	-	11.1	8.3	-	8.3
#2	16.7	-	16.7	11.1	-	11.1	8.0	-	8.0
#3	16.7	-	16.7	11.1	-	11.1	7.6	-	7.6
				Pile Tests					
#5	26.8	44.6	71.4	18.3	44.6	62.9	10.0	49.2	59.2
#6	27.4	55.8	83.2	19.1	55.8	74.9	10.0	54.7	64.7
#7	27.9	66.9	94.8	19.8	66.9	86.7	12.0	60.7	72.7

Table 11. (Continued)

Per Cent Measured of Calculated (General Shear Failure)			Per Cent Measured of Calculated (Local Shear Failure)		
Point	Side	Total	Point	Side	Total
		Surface Tests			
49.7	-	49.7	74.7	-	74.7
47.9	-	47.9	72.0	-	72.0
45.5	-	45.5	68.5	-	68.5
		Pile Tests			
37.3	110.2	83.0	54.6	110.2	94.2
36.5	98.1	77.8	52.4	98.1	86.5
43.0	90.9	76.7	60.6	90.9	83.9

Table 12. Measured Skin Friction

Test	Side Friction (pounds)	Measured Skin Friction Surface Area (in^2)	Skin Friction (lbs/in^2)
#5	49.2	100.5	0.490
#6	54.7	125.7	0.436
#7	60.7	150.8	0.404

Average Measured Skin Friction = 0.443 lbs/in^2

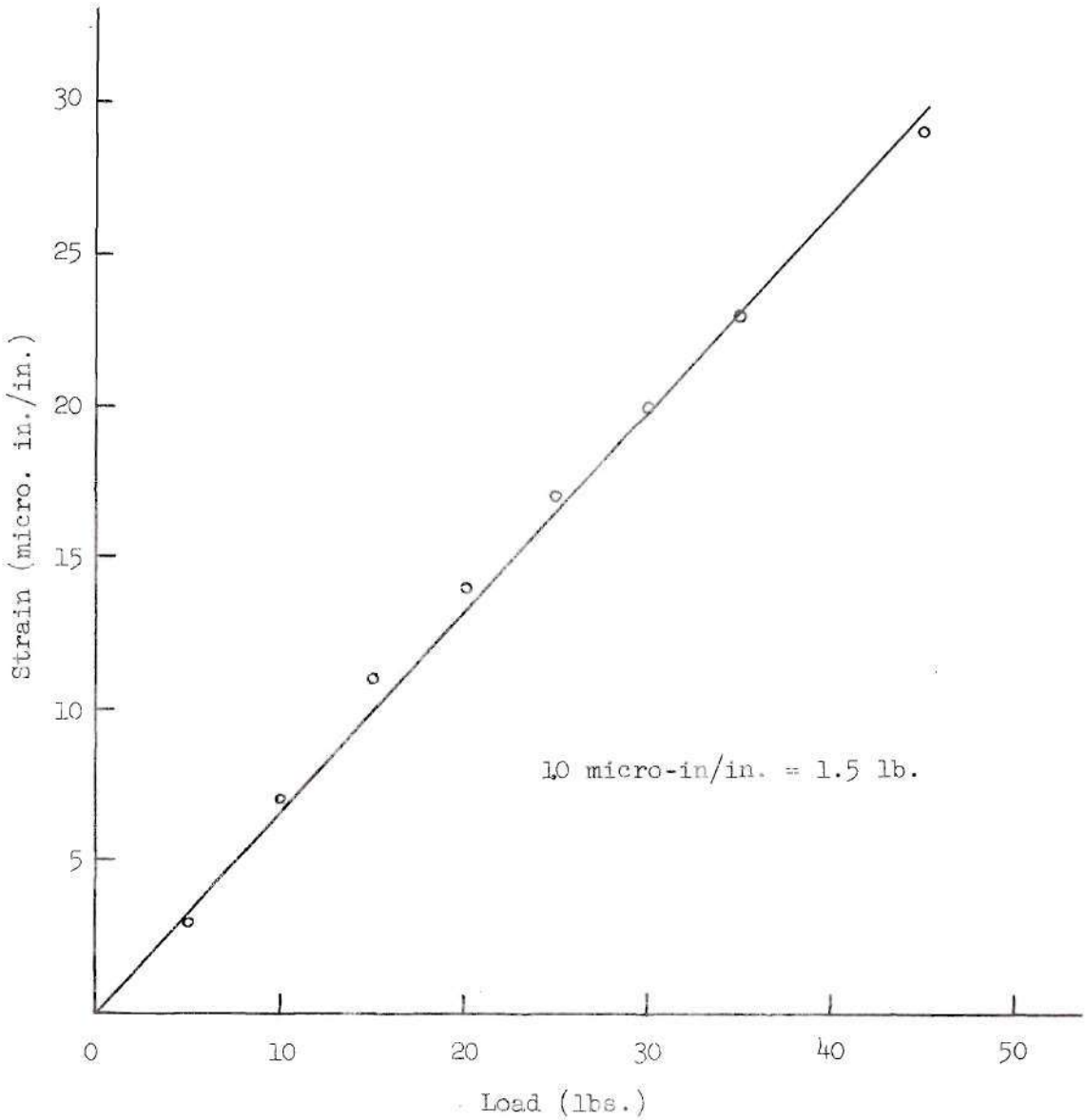

Figure 7. Calibration Curve

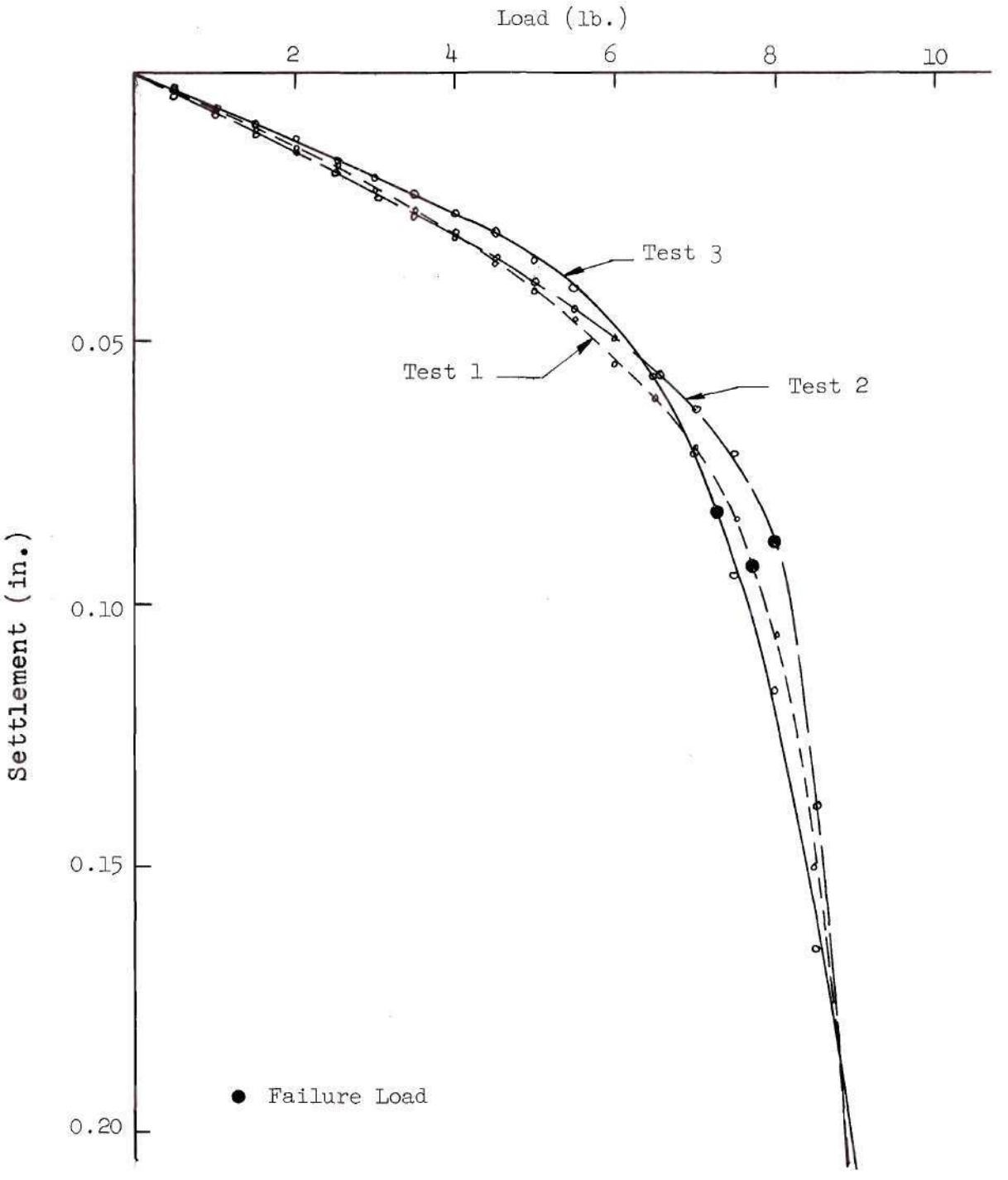

Figure 8. Surface-Load Settlement Curves

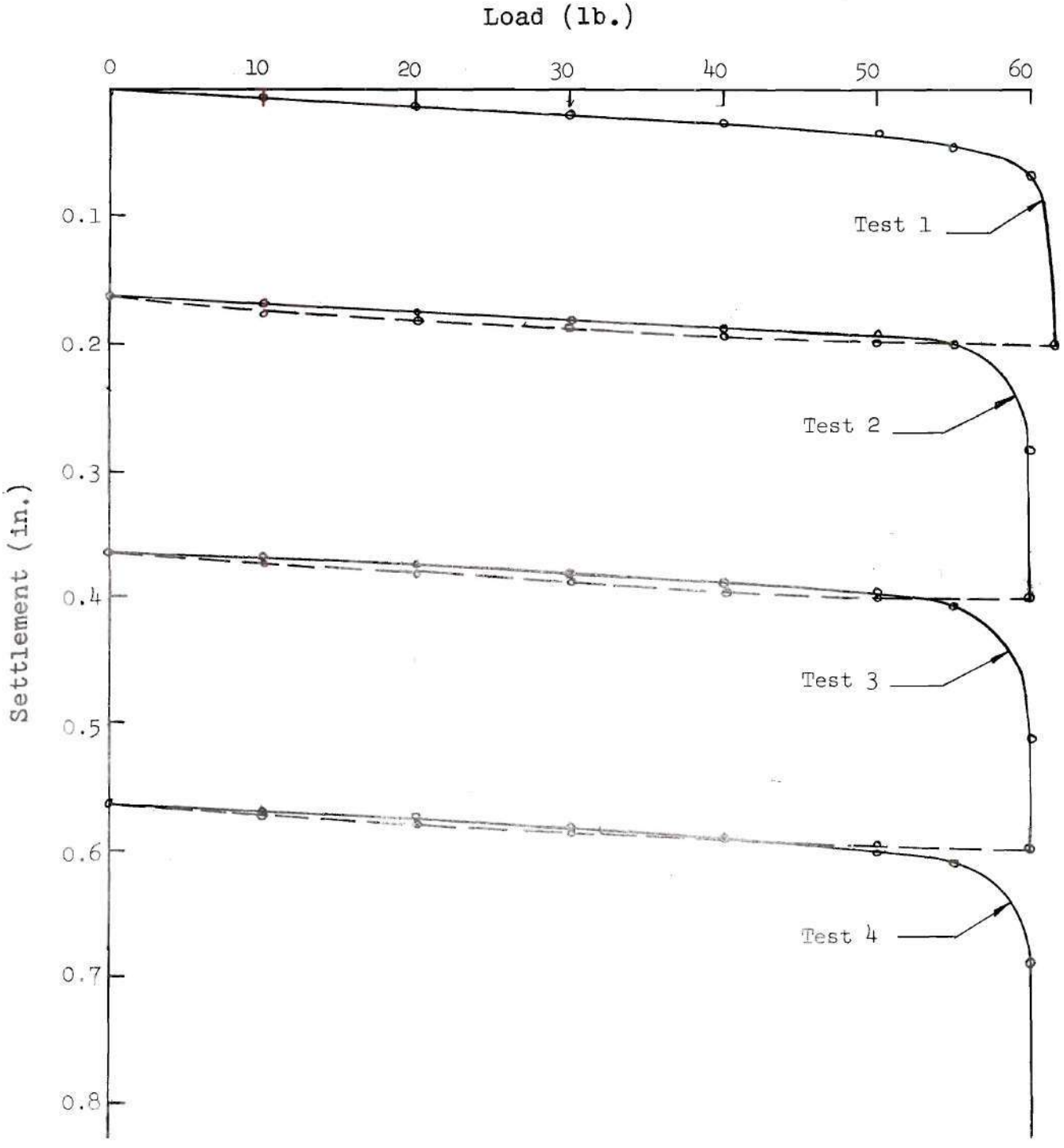

Figure 9. Pile Load-Settlement Curves
(Observation of Failure Surface)

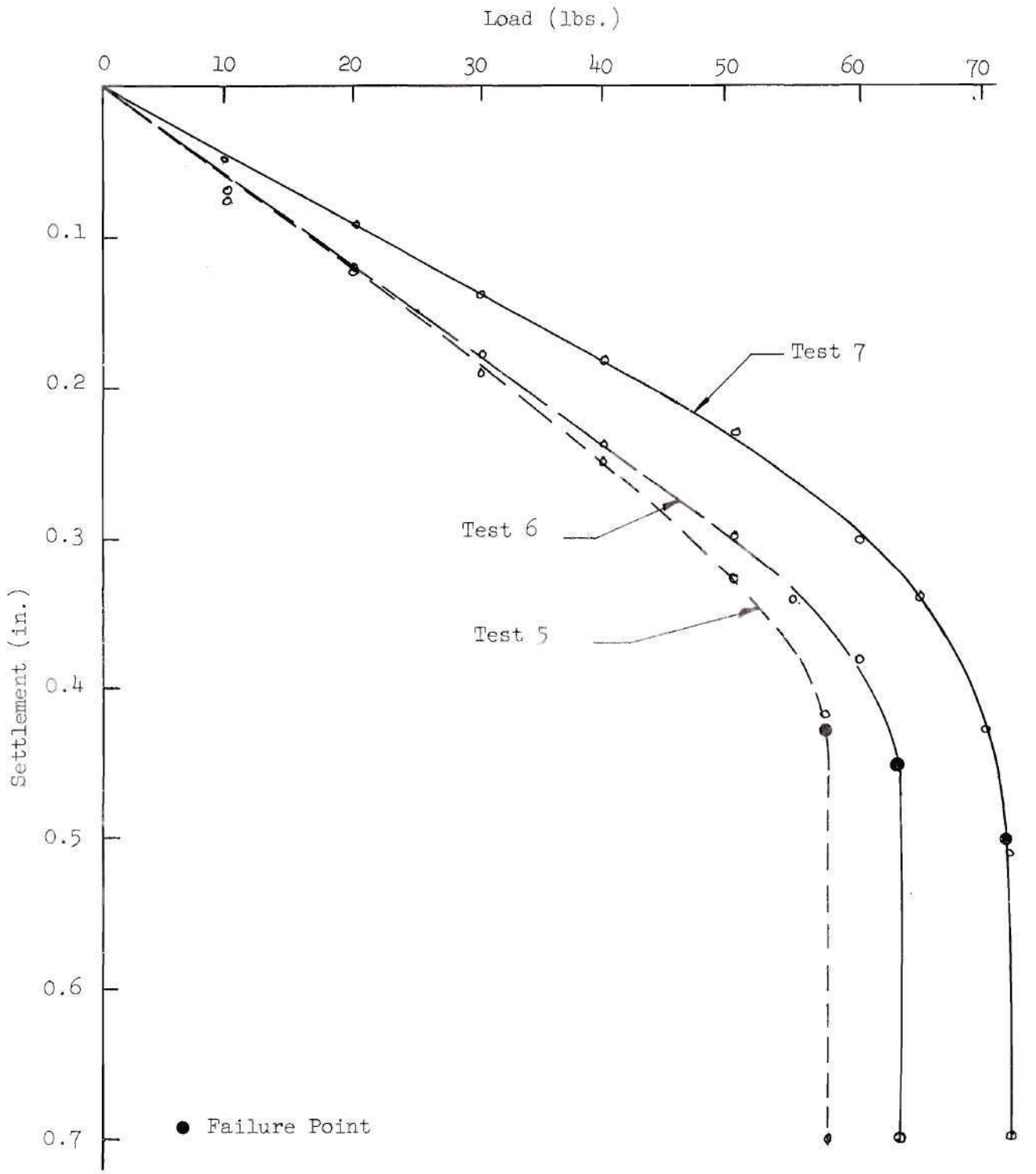

Figure 10. Pile Load-Settlement Curves:
(Determination of End Load)

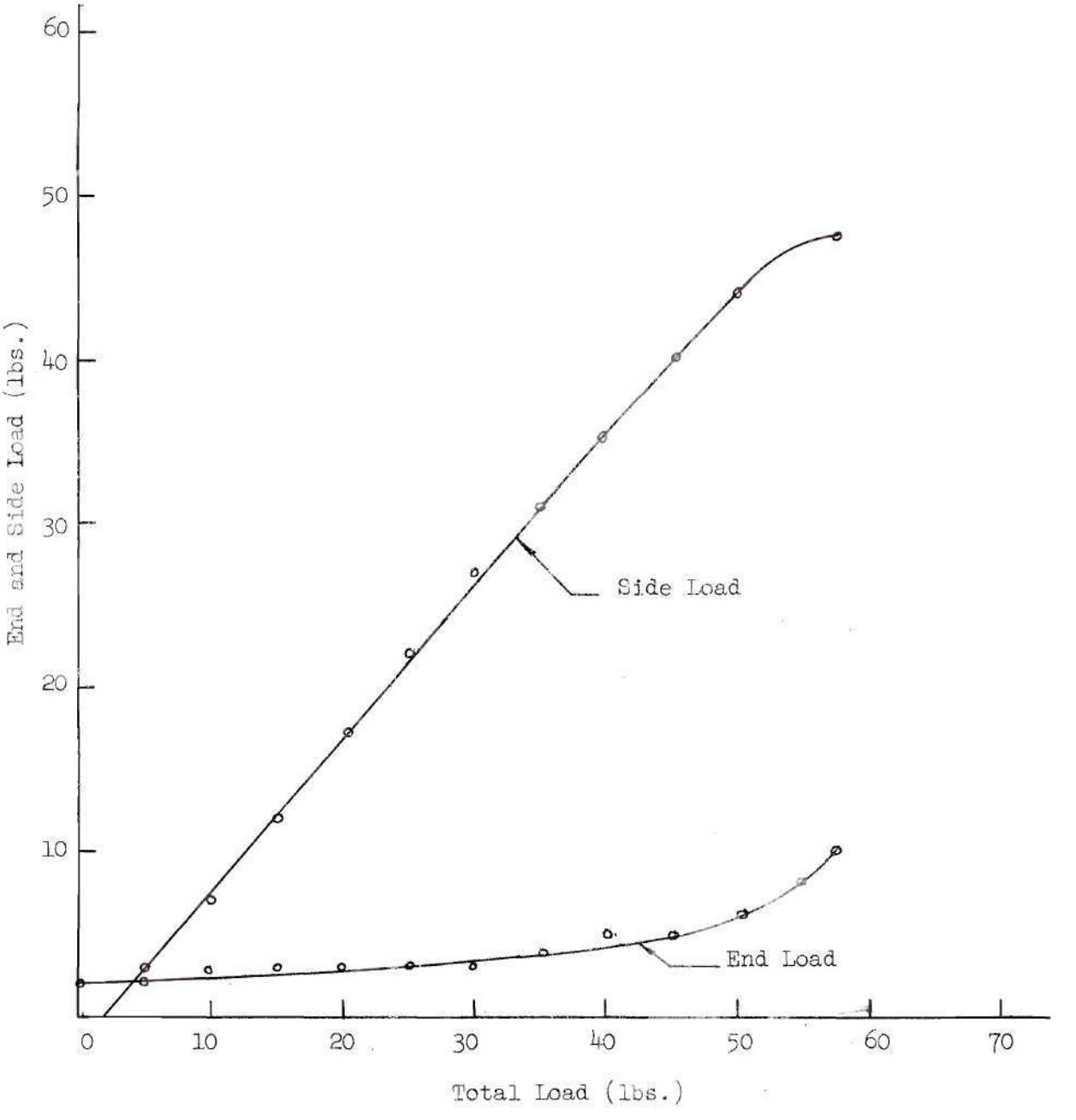

Figure 11. Pile Load Distribution: Pile Test 5

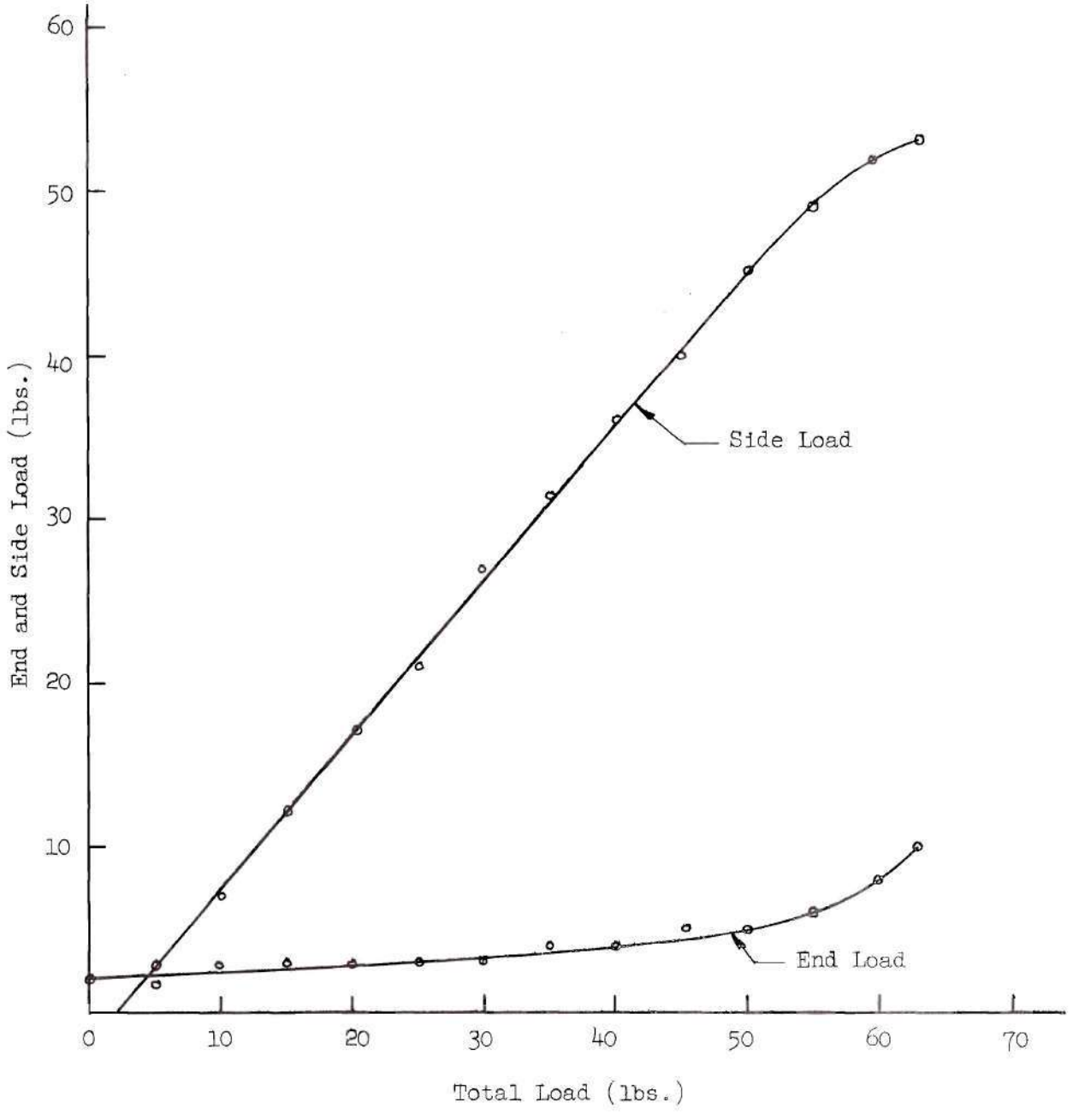

Figure 12. Pile Load Distribution: Pile Test 6

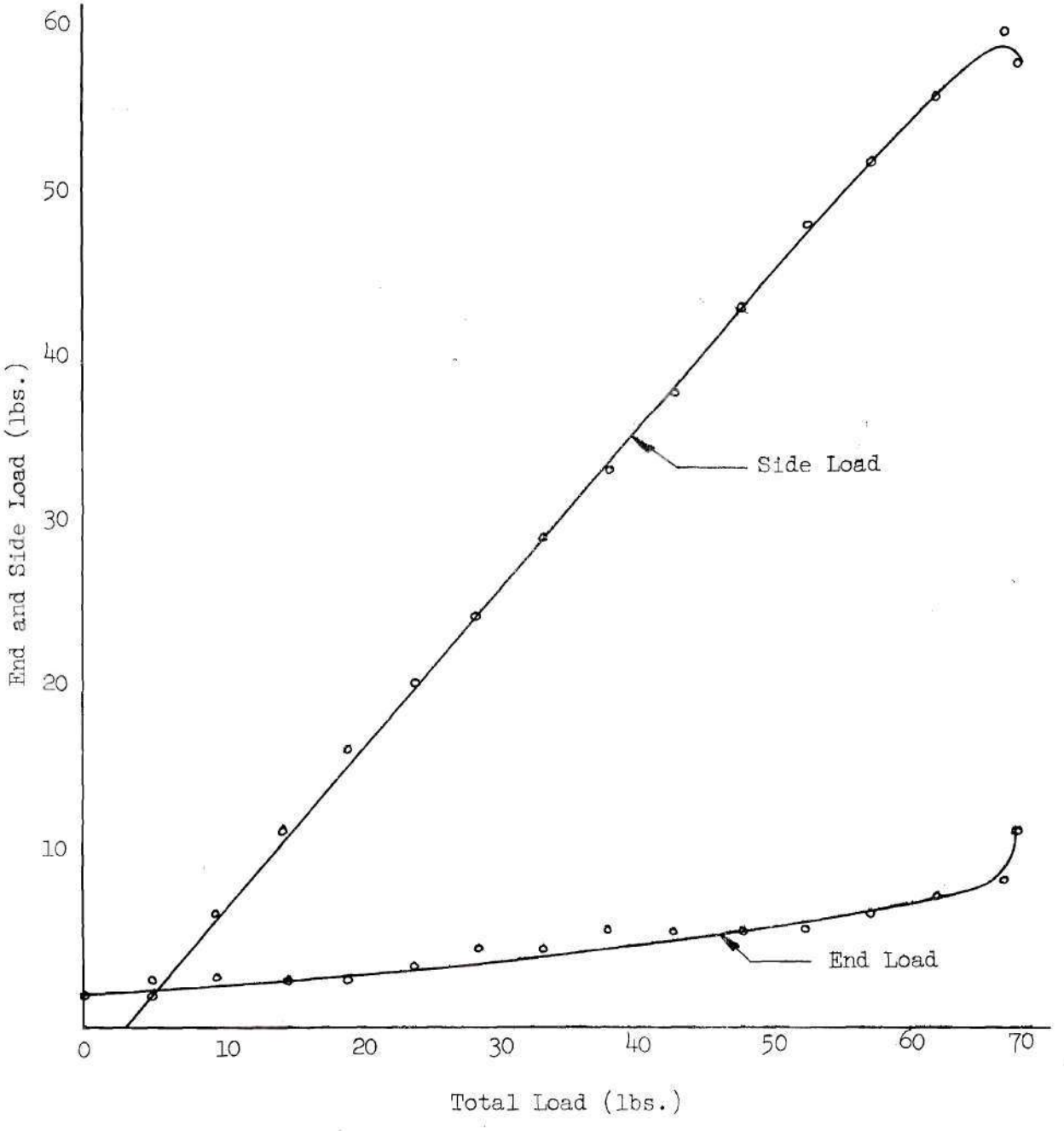

Figure 13. Pile Load Distribution: Pile Test 7

BIBLIOGRAPHY

Literature Cited

1. Meyerhoff, G. G., "The Ultimate Bearing Capacity of Foundations," Geotechnique, Vol. II, No. 4. London: Hollen Street Press, Ltd., 1951, pp. 301-332.

2. Terzaghi, Karl, Theoretical Soil Mechanics, New York: John Wiley and Sons, Inc., Ninth Printing, 1959, p. 118.

3. Ibid., p. 136.

4. Meyerhoff, op. cit., pp. 301-332.

5. Sowers, G. F., "Piles in Cohesive Material," Proceedings of the Fifth International Soil Conference, 1961, Vol. 2.

6. Bishop, R. F., Hill, R. and Mott, N. F., "The Theory of Indention and Hardness Test," Proceedings of the Physical Society, Vol. 57, The Physical Society, 1949, p. 147.

7. Seed, H. Bolton and Lyman C. Reese, "The Action of Soft Clay Along Friction Piles," Transactions, American Society of Civil Engineers, Vol. 122, 1957, pp. 735-737.

8. Wilson, Lyle Lawrence, Model Studies of the Load Distribution Within Groups of Friction Piles in a Cohesive Soil. Unpublished M. S. Thesis, School of Civil Engineering, Georgia Institute of Technology, 1957, p. 34.

9. Seed, op. cit., pp. 735-737.

10. Wilson, op. cit., p. 10.

11. Terzaghi, op. cit., p. 120.

12. Fausold, Howard Marshal, Model Studies of Pile Bearing Capacity Relationships in a Cohesive Soil. Unpublished M. S. Thesis, School of Civil Engineering, Georgia Institute of Technology, pp. 13-18.

13. Ibid., pp. 32-38.